


Apparent timing of density banding in the Caribbean coral *Siderastrea siderea* suggests complex role of key physiological variables

B. E. Benson^{1,2}  · J. P. Rippe³ · C. B. Bove¹ · K. D. Castillo^{1,3}

Received: 13 May 2018 / Accepted: 13 November 2018 / Published online: 17 November 2018

Abstract Skeletal growth bands in massive reef-building corals are increasingly used as proxies for environmental records despite an incomplete understanding of their formation. While the bands are known to arise from seasonal changes in light and temperature, conflicting reports about the timing of constituent high- and low-density growth bands have complicated the dating and interpretation of environmental signals recorded in corals' growth histories. Here, we analyze 35 *Siderastrea siderea* cores extracted from inshore and offshore reef zones along the Florida Keys Reef Tract to investigate potential drivers of banding variability in this species. A previously proposed model of banding variation is applied to assess its potential to explain band timing in *S. siderea*. Colony growth characteristics and the timing of band deposition were obtained from the cores via computed tomography and were coupled with tissue thickness measurements and gender identification. Apparent time difference, or the perceived lag in coral growth response to changes in environmental conditions, was quantified for each coral core. Results suggest that

linear extension, tissue thickness, and gender together do not fully explain the timing of band formation in *S. siderea* and therefore do not fully resolve the density patterns observed within this species. This finding suggests that other factors yet to be identified are partially determining the formation and appearance of density bands in *S. siderea*. The continued characterization of banding variability on scales ranging from the individual colony to entire reef systems will enrich our understanding of both coral growth and the environmental conditions to which corals are exposed.

Keywords Coral growth · Density banding · *Siderastrea siderea* · Proxy data

Introduction

As early as 1890, researchers observed that certain biological and geochemical features within organisms record information about the environments to which they are exposed (Smalley and Fagg 2015). These records—often stored in the form of isotopes, growth patterns, and inclusions—can subsequently be recovered and analyzed for information about past environmental conditions (Barnes and Lough 1996). The resulting information is collectively referred to as proxy records and has informed our understanding of phenomena ranging from global glacial cycles (Wolff et al. 2006; Williams et al. 2009; Haberlah et al. 2010) to rainfall patterns in equatorial East Africa (Verschuren et al. 2000). However, traditional sources of high-frequency proxy records like that of temperate tree rings poorly represent the tropics, and instrumental data in these lower latitude regions are often lacking (Hurrell et al. 2006). Thus, available data are insufficient for a complete

Topic Editor Morgan S. Pratchett

Electronic supplementary material The online version of this article (<https://doi.org/10.1007/s00338-018-01753-w>) contains supplementary material, which is available to authorized users.

✉ B. E. Benson
bebenson9@gmail.com

¹ Environment, Ecology, and Energy Program, University of North Carolina at Chapel Hill, Chapel Hill, NC, USA

² Department of Biology, Boston University, 5 Cummington Mall Rm. 217, Boston, MA 02215, USA

³ Department of Marine Sciences, University of North Carolina at Chapel Hill, Chapel Hill, NC, USA

understanding of paleoclimatic environments and phenomena, and such a lack of robust data on changes over geologic timescales limits our ability to predict and understand current and future climate changes (Langebroek et al. 2012).

When the annual nature of growth bands in massive scleractinian corals was established in 1972, researchers recognized the potential for these bands to provide climate data where ice cores and tree rings could not (Knutson et al. 1972; Lough et al. 1996). Early investigators posited that the alternating high- and low-density band couplets reflect annual light and temperature cycles (Knutson et al. 1972; Highsmith 1979; Barnes and Lough 1993). Other factors like latitude, rainfall, freshwater runoff, and sea level pressure may influence banding patterns, though their impacts are less well understood (Highsmith 1979; Dodge and Vaisnys 1980; Lough and Barnes 1989, 2000; Barnes et al. 2003). The bands, found within the coral's calcium carbonate skeleton, can be visualized with relative ease using X-radiography (Knutson et al. 1972), and the ubiquity of these shallow-water tropical corals has made possible the measurement and interpretation of growth patterns over temporal and spatial gradients (Buddemeier et al. 1974; Highsmith 1979; Hubbard and Scaturro 1985). More recently, the density bands have enabled characterization of coral responses to ocean warming (Cantin et al. 2010; Castillo et al. 2012). Despite the accepted link between environmental conditions and variations in core density, the exact timing of the formation of each semiannual band remains unclear for most coral species (Brown et al. 1986; Barnes and Devereux 1988; Lough and Barnes 1990; Winter et al. 1991; Barnes and Lough 1993).

Many studies have concluded that high-density bands are deposited at times of maximum temperature (generally summer), while low-density bands are deposited during periods of lower temperature in the winter (see Lough and Barnes 1990 for a review). However, cores extracted from corals days and kilometers apart often present opposite bands at the apex of the core—the position on which all banding chronologies rely for backdating (Lough and Barnes 1990; Barnes and Lough 1993; Taylor et al. 1993; Carricart-Ganivet et al. 2013). Without a consistent framework through which researchers can contextualize these contrasting patterns, variability in banding cannot be reliably parsed into its environmental and genotypic determinants.

To help resolve these inconsistencies and explain variability in banding, Taylor, Barnes, and Lough developed a simple model of density band formation in corals based on observations of *Porites* spp. from the Great Barrier Reef (Barnes and Lough 1993; Taylor et al. 1993). The *Porites* spp. work suggested that skeletal growth in this genus can be attributed to three main processes: monthly tissue uplift,

linear extension at the outermost surface of the colony, and skeletal infilling throughout the depth of the tissue layer, termed thickening (Barnes and Lough 1993). A mathematical model based on the *Porites* spp. observations, termed the Townsville model, determined that the perceived displacement between an environmental signal and the resulting record in the coral skeleton—the apparent time difference, or ATD—varies with the ratio between tissue thickness and linear extension. This displacement can be measured by directly calculating the apparent temporal lag between an environmental signal (e.g., summer maximum temperature) and the resulting signature (e.g., maximum annual density) in the banding profile, relative to the most recently deposited semiannual band in an extracted core. The importance of tissue thickness and extension rate in determining the degree of displacement is a consequence of the fact that, while the coral responds to changes in environmental conditions (i.e., sinusoidal light and temperature cycles) in real time, the resulting calcification largely occurs beneath the skeletal surface, throughout the depth of the tissue layer (Knutson et al. 1972; Highsmith 1979; Barnes and Lough 1993; Taylor et al. 1993). Accounting for how between-colony differences in tissue thickness and extension rate alter the presentation of the bands allows for a more targeted examination of the relationship between banding and environmental drivers. Furthermore, knowing the tissue thickness and extension rate of a colony can inform predictions of ATD under a given suite of environmental conditions.

In the current study, the Townsville model was applied to the massive reef-building Caribbean coral *Siderastrea siderea*. Members of this species are long-lived, thermally tolerant, common throughout the Caribbean, and slow-growing, making them excellent candidates for proxy data (Guzmán and Tudhope 1998; Castillo et al. 2011, 2012). Proxy data found within this coral has hitherto been used to study several elements of past climate across the Caribbean, including reductions in upwelling off the coast of Venezuela (Reuer et al. 2003) and sea surface temperature variability in the Gulf of Mexico (DeLong et al. 2014). Yet, without a clear and reliable understanding of the banding pattern variability in *S. siderea* along with its drivers, proxy data remain limited in resolution to processes that can be observed on annual to decadal scales. To investigate the applicability of the Townsville model in *S. siderea*, 35 cores were analyzed from four paired inshore and offshore sites (eight total sites) along the Florida Keys Reef Tract (FKRT). Predicted values of ATD (ATD_p) were calculated for each core by measuring tissue thickness and extension rate as described in the Townsville model (Taylor et al. 1993). Predicted ATD was subsequently compared with ATD values obtained from each core's banding profile as

well as known physiological drivers of growth and banding.

Methods

Coral core extraction

Cores of *S. siderea* were extracted from four paired inshore and offshore sites along the FKRT between April 2015 and May 2016 (Fig. 1, Table 1; Section A, ESM). Coral cores were extracted from apparently healthy colonies at 3–6 m depth. Cores 5 cm in diameter were extracted along the maximum vertical growth axis of each coral colony by SCUBA divers using a handheld hydraulic core drill (*CS Unitec; Norwalk, Connecticut*) with a hollow extension rod and wet diamond core bit. Drilling was extended to the base of the colony whenever possible to obtain complete growth chronologies for each core. Following extraction, a concrete plug was inserted into the drilled holes and sealed with underwater epoxy to minimize bioerosion. Extracted cores were rinsed in 95% ethanol and transported to the University of North Carolina at Chapel Hill (UNC) in polyvinyl chloride tubes for analyses.

Core digital reconstruction and annual growth measurements

Coral cores were scanned using a Siemens Biograph64 CT scanner (*Siemens Medical Solutions, Erlangen, Germany*) at the UNC Biomedical Research Imaging Center to obtain images with 10 mm slice thickness and 0.6 mm pixel spacing. Digital three-dimensional reconstructions of the cores were created in Horos v1.1.7 (*Purview, Annapolis, MD, USA*) from the CT images. Minimum intensity projections (minIP) across a 10-mm-thick section through the center of each reconstructed core were used to visualize density bands. MinIP images were preferred over mean projection images due to unclear banding patterns in the latter (Section B, ESM).

For each core, three linear transects along the axis of growth were drawn to obtain Hounsfield values, which measure linear X-ray attenuation (Hounsfield 1973). Hounsfield units were converted to bulk density (g cm^{-3}) using a standard curve generated from coral skeleton samples of known density. The transects were then averaged together to create a single banding profile for each core that depicted changes in minimum density (simply ‘density,’ hereafter) within the core and the timing of extrema. Annual linear extension (cm yr^{-1}) represented the

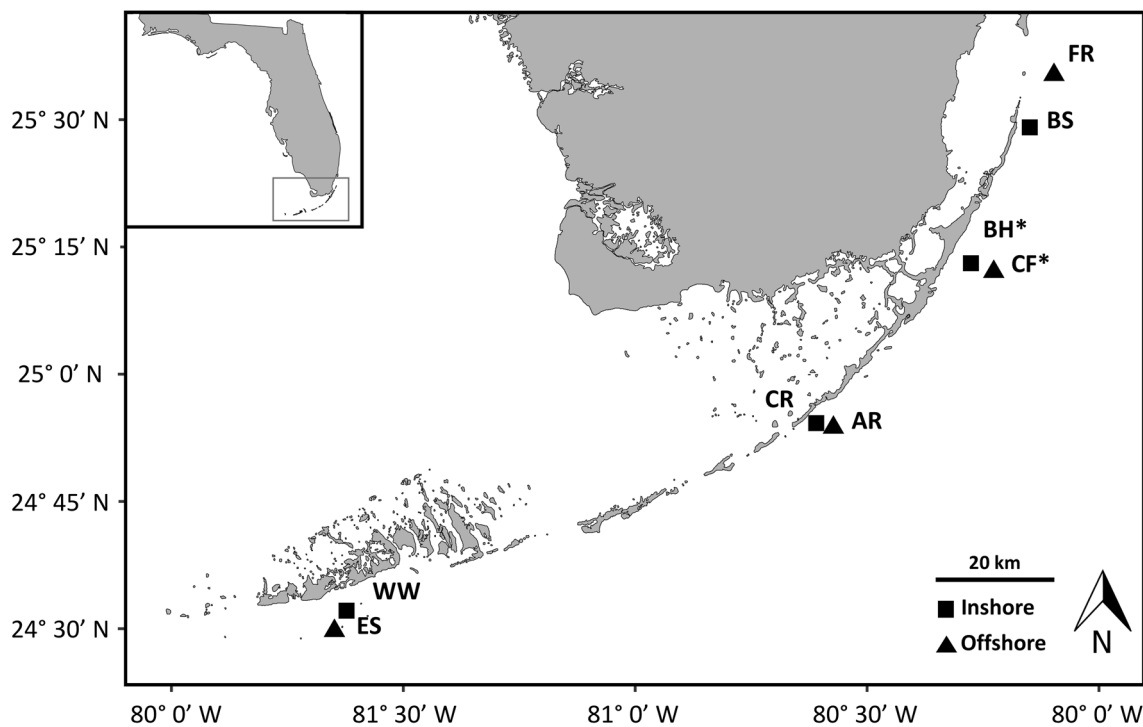


Fig. 1 Map of *Siderastrea siderea* core extraction sites. Inshore sites (squares): West Washerwoman (WW), Cheeca Rocks (CR), Basin Hill Shoals (BH), and Bache Shoals (BS). Offshore sites (triangles): Eastern Sambo (ES), Alligator Reef (AR), Carysfort Reef (CF), and Fowey Rocks (FR). Tissue microsamples for histological analysis

were collected from all sites except for BH and CF (indicated with *). Map layer from the National Oceanic and Atmospheric Administration’s Global Self-consistent, Hierarchical, High-resolution Geography Database (Wessel and Smith 1996)

Table 1 Physiological measurement means (\pm SE) across the 8 sampling sites

Site	Code	Zone	n	Length (cm)	Tissue (mm)	E_0 (mm yr ⁻¹)	E_1	(M, F)
All sites	–	–	35	37.53 (\pm 2.55)	6.35 (\pm 0.14)	3.54 (\pm 0.14)	0.86 (\pm 0.03)	6, 8
Fowey Rocks	FR	Offshore	3	23.93 (\pm 6.78)	6.67 (\pm 0.59)	3.44 (\pm 0.37)	0.84 (\pm 0.04)	0, 0
Carysfort Reef	CF	Offshore	5	32.26 (\pm 3.23)	6.44 (\pm 0.21)	3.96 (\pm 0.42)	0.87 (\pm 0.09)	NA
Alligator Reef	AR	Offshore	4	23.83 (\pm 4.68)	6.56 (\pm 0.08)	3.23 (\pm 0.57)	0.81 (\pm 0.12)	2, 1
Eastern Sambo	ES	Offshore	5	49.78 (\pm 4.37)	5.87 (\pm 0.37)	3.41 (\pm 0.27)	0.85 (\pm 0.03)	0, 3
Bache Shoals	BS	Inshore	4	34.03 (\pm 5.29)	6.65 (\pm 0.58)	3.36 (\pm 0.50)	0.92 (\pm 0.04)	1, 1
Basin Hill Shoals	BH	Inshore	5	38.86 (\pm 6.87)	6.10 (\pm 0.52)	3.60 (\pm 0.60)	0.83 (\pm 0.04)	NA
Cheeca Rocks	CR	Inshore	5	58.42 (\pm 4.40)	6.26 (\pm 0.42)	3.61 (\pm 0.31)	0.91 (\pm 0.09)	1, 1
West Washerwoman	WW	Inshore	4	28.45 (\pm 3.55)	6.49 (\pm 0.35)	3.54 (\pm 0.27)	0.88 (\pm 0.11)	2, 2

Data columns from left to right: full site name, two-letter site code, reef zone type, number of cores collected, mean core length, tissue thickness, extension rate (E_0), variation in annual extension or the ratio of winter to summer extension rates (E_1), and the number of male (M) or female (F) colonies identified from each site

sum of paired semiannual high-density (HD) and low-density (LD) bands. Linear extension estimates were restricted to the most recent 5 yr of extension within each core to reduce the influence of interannual variability in tissue thickness and extension rate on modeled relationships between variables. The most recently deposited band at the top of each core was determined using the digital reconstructions, and a Fisher's exact test was used to test for independence of gender and most recent band. All statistical analyses of these relationships were implemented in R 3.4.3 (R Core Team 2017).

Physiological measurements

Several physiological characteristics thought to influence banding were assessed, including colony size (via core length, per Barnes and Lough 1992), collection site (Barnes and Lough 1992), reef zone (Castillo et al. 2011, 2012), extension rate (E_0 , Barnes and Lough 1993; Taylor et al. 1993), variation in extension rate (E_1 , Barnes and Lough 1993; Taylor et al. 1993), tissue thickness (TTL , Barnes and Devereux 1988; Barnes and Lough 1993; Taylor et al. 1993), and gender (Carricart-Ganivet et al. 2013; Mozqueda-Torres et al. 2018). Core length (cm) was measured using a tape measure to determine the maximum length from the top of each core to its base. During coring, significant effort was made to drill to the base of each colony to ensure that core length is a good approximation of colony size. Approximate tissue thickness (mm) was measured using a digital caliper from the top of each core to the part of the core where the extent of a dark stain is still visible from the remains of living tissue (Barnes et al. 2003, Fig. 2). Core length, thickness of the tissue layer (TTL), and mean annual extension rates (E_0) were compared between sites and reef zones to assess geographic

variability in these key phenotypic variables using pairwise linear regression, and Tukey's HSD test was used to explore any significant differences (R *stats* package, R Core Team 2017).

Gender determination

Tissue microsamples for gender determination were collected in April 2016 from 28 cored colonies across six of the eight sampling sites (Fig. 1). Microsamples were taken near the core extraction point at the apex of the colony and kept alive in seawater during transport to UNC. At UNC, fragments were fixed in 95% Zenker's solution with 5% formaldehyde prior to decalcification in a 10% HCl solution following Glynn et al. (1991) until skeletal dissolution was complete. Decalcified tissue samples were preserved in 70% EtOH prior to processing by the UNC Histopathology Core. In preparation for mounting, samples were dehydrated using a series of reagent alcohols, cleared with xylene, and infiltrated with paraffin. Samples were then sectioned longitudinally at 4 microns and stained using a Leica ST5010 Autostainer XL (*Leica Biosystems*) following the hematoxylin and eosin stain method (Fischer et al. 2008). Dry, slipcovered slides were returned to the laboratory where gamete determination was conducted using light microscopy to identify spermaries and oocytes (Szmant 1986). Because tissue fragments were collected prior to peak annual spawning time, gametes were not present in all individuals (Szmant 1986; St. Gelais et al. 2016). Only those samples for which gametes could be positively identified were included in the gender analyses ($n = 14$; 6 male, 8 female). Pairwise linear regression was used to evaluate relationships between gender and core length, TTL , E_0 , and E_1 (R *stats* package, R Core Team 2017).

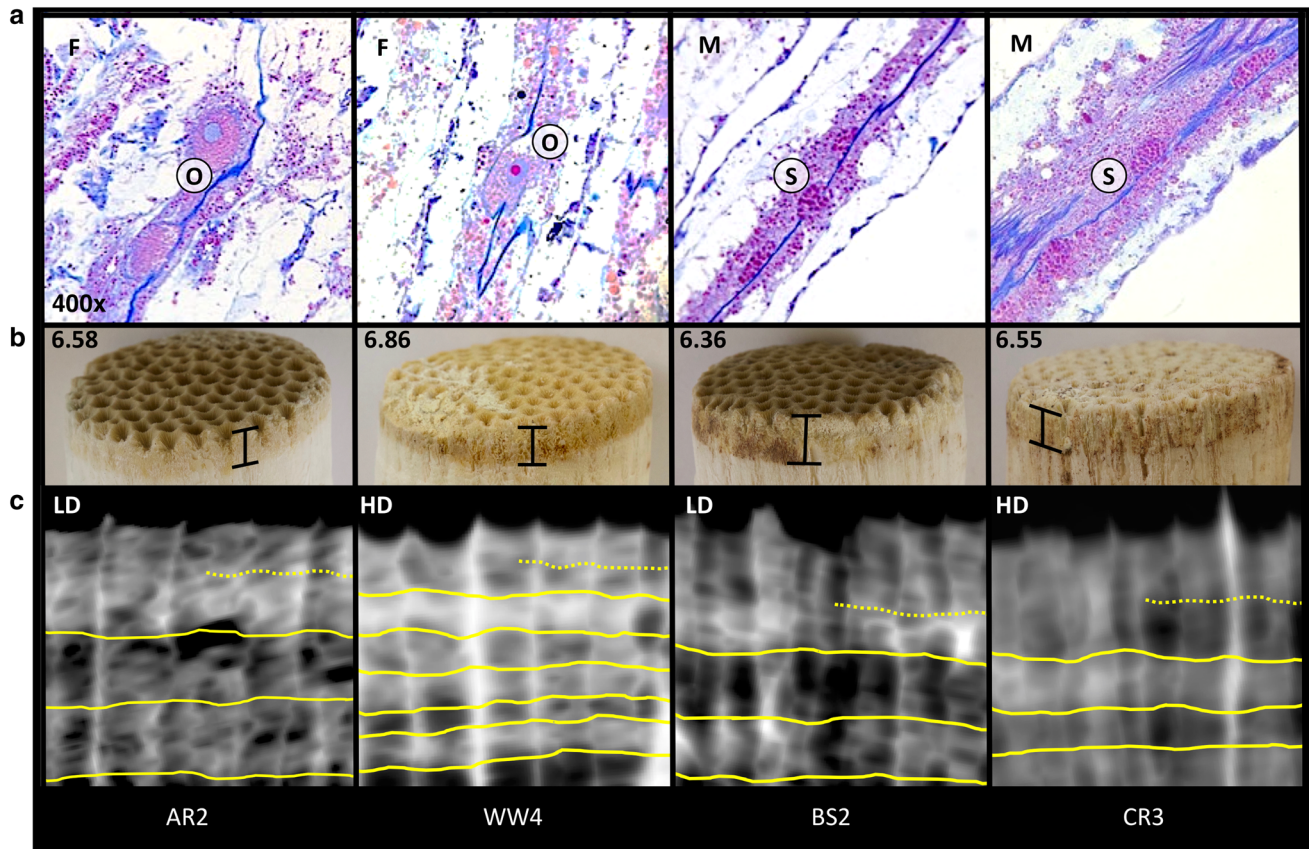


Fig. 2 **a** Histological slide images ($\times 400$) from four individual corals in the present study (left to right: AR2, WW4, BS2, CR3). 'F' and 'M' are female and male, respectively, while oocytes are marked by 'O' and spermaries are marked by 'S.' **b** Corresponding tissue thicknesses (mm) measured at the top of the core. Capped black bars represent measured tissue thickness based on measurements at 6 locations around each core's apex. **c** Computed tomography (CT)

images depicting the most recently deposited band of each core and several previously deposited bands. Horizontal yellow lines demarcate high-density (HD) and low-density (LD) bands. The top band (annotated HD or LD) is indicated by the dashed yellow line, half of which is omitted. Controlling for similar tissue thicknesses, these individuals demonstrate all possible combinations of colony gender and most recent band

Predicted apparent time difference

Predicted apparent time difference (ATD_P), or the predicted difference between a peak in environmental conditions and a corresponding peak in core density (see Table 2

for explanation of terminology), was calculated in months according to the equation:

$$\text{Apparent time difference} = 12 \times \left(\left[\frac{TTL/E_0}{2} \right] + \frac{E_1}{2\pi} \sin \pi TTL/E_0 \right)$$

Table 2 Differentiation between the various types of apparent time difference (ATD) as discussed in the current study as well as in Taylor et al. (1993)

Acronym	Measure of ATD	Source
ATD	Apparent time difference: a general term referring to the apparent displacement in time and distance within a coral core between a peak (trough) in an environmental signal and a corresponding peak (trough) in coral density	Taylor et al. (1993)
ATD_P	Apparent time difference as predicted by the Townsville model	Taylor et al. (1993)
ATD_{O-T}	Apparent time difference as measured in the cores of this study in relation to SST	Current study
ATD_{O-P}	Apparent time difference as measured in the cores of this study in relation to PAR	Current study
ATD_M	Apparent time difference as given by the averaged model in this study	Current study

where 12 is the number of months in a year and the sine function represents a reasonable approximation for seasonal variations in environmental conditions (Taylor et al. 1993). Variable E_1 was calculated as the ratio of minimum winter extension (generally associated with LD bands) to maximum summer extension (HD bands) per Taylor et al. (1993). Semiannual extension rates of LD and HD bands were obtained as the length in pixels of each band within the minIP images in Horos to calculate the E_1 ratio (Table S1, ESM). Several values of ATD_P in our core set exceeded 12 months (14 of 35 cores); in other words, several corals exhibited a predicted ≥ 1 yr displacement between an environmental signal and the corresponding density signature in the coral's growth record. Though values exceeding 12 months are biologically possible, the banding pattern will appear to exhibit the same degree of displacement from the environmental forcing function as the pattern of a core with an ATD of 12 fewer months; i.e., two cores collected at the same time with measured ATDs of 12 months and 24 months will appear to have deposited their most recent band at the same point within the 12-month annual temperature profile. Therefore, predicted apparent time difference was constrained such that $0 < ATD_P < 12$ by subtracting 12 from values exceeding 12 months to facilitate comparison with observed apparent time difference, which was measured on a scale of 0–12 months.

Observed apparent time difference

Observed apparent time difference (ATD_O) was calculated separately using two different environmental drivers to investigate which might be more tightly linked with ATD_O . First, ATD_O was calculated by comparing 5-yr profiles of core density and sea surface temperature, termed ATD_{O-T} (SST; Reynolds et al. 2007). Second, it was calculated by comparing the same 5-yr profiles with photosynthetically available radiation, termed ATD_{O-P} (PAR; NASA 2018). For both SST-derived and PAR-derived ATD_O , density profiles extracted from Horos were standardized on an annual scale such that the number of pixels in an annual HD and LD band couplet always represented 365 days. Time-standardized banding profiles were then plotted against the environmental driver signal from the collection site at daily resolution (Fig. S1, ESM). ATD_O was defined as the temporal distance in months between a peak in the environmental driver and a corresponding peak in core density (Table 2), with the core extraction date serving as a reference for backdating. ATD_O was always recorded as the displacement between the most temporally proximate matching extremes (peak-to-peak) in density and the environmental forcing functions to maximize the number

of replicates that could be extracted from 5-yr banding profiles (Section C, ESM). In some cases, this method led to substantially different ATD_O values between forcing functions when ATDs were close to zero or twelve months, and these values were transformed using a 1-period shift (± 12 months) to facilitate comparison (Section D, Figs. S2–S3, ESM). Pairing density extrema with environmental driver minima (as is observed in some species; Lough and Barnes 1990) did not change the results of the model (Section C, ESM), and hence, all cores were analyzed using paired matching extrema.

Comparison of 5-yr ATD versus ATD of the most recent extreme

Five-year profiles of banding were preferred in the current study to allow for within-core replication of ATD estimates. However, the further back in the core that ATD is calculated, the greater the influence of age model errors (Comboul et al. 2014). To assess the potential influence of age model errors on ATD, ATD_O was also calculated both in reference to SST and PAR using only the most recent extreme in density beneath the incompletely formed top-most band. The difference in means between these two approaches to ATD was assessed using one-way ANOVAs (R *stats* package, R Core Team 2017).

Evaluation of the Townsville model

A zero-method model averaging approach (Burnham and Anderson 1998) was used to evaluate the applicability of the Townsville model to *S. siderea* (Taylor et al. 1993). This approach is well suited for studies that aim to elucidate which factors have the strongest influence on a response variable in complex ecological systems (Nakagawa and Freckleton 2011; Grueber et al. 2011). Specifically, the relative contribution of each characteristic of growth, physiology and geography to ATD_{O-T} and ATD_{O-P} was assessed using global models that included the Townsville variables (TTL , E_0 , and E_1) as interactive effects, *Core Length* as an additive effect and *Site* as a random effect nested within *Reef Zone*. This was achieved by utilizing the *MuMIn* (Bartón 2013), *arm* (Gelman and Su 2018), and *lme4* (Bates et al. 2015) packages in R (R Core Team 2017). Relative importance of each physiological variable in determining ATD_P was estimated by summing the weights of component models in which a given variable appears in the model averaging output. Effect sizes, or the standardized parameter estimate for a particular variable, were obtained for both ATD_{O-T} and ATD_{O-P} . Additional information about model selection can be found in Section E of the ESM.

Finally, pairwise linear regression was used to evaluate agreement between ATD_P and observed values (ATD_{O-T} and ATD_{O-P}) as well as ATD_P and modeled values (model outputs). Note that unconstrained values of ATD_P were used when relating ATD_P to modeled values, as constrained values may interfere with the ability to detect a correlation between these.

Results

Coral growth and physiological measurements

Mean (\pm SE) core length across all sites was 37.53 (\pm 2.55) cm (Table 1). Core length ($n = 38$) differed significantly between sites ($p < 0.001$) but not reef zone ($p = 0.128$). A post hoc Tukey's HSD test revealed that Cheeca Rocks and Eastern Sambo were driving this difference, each with several significant pairwise p values ($p < 0.05$, Table S2, ESM). In contrast to core length, other variables (TTL , E_0 , E_1 , ATD_P , ATD_O) were not significantly different by site or reef zone. E_1 in particular appeared to be stable both within and across sites with an overall mean (\pm SE) value of 0.86 (\pm 0.03). Mean (\pm SE) TTL for all cores was 6.35 (\pm 0.14) mm, while mean (\pm SE) E_0 was 3.54 (\pm 0.14) mm yr⁻¹.

Gender differences

Gametes were found in 14 of 28 tissue samples ($n = 8$ female, 6 male; Fig. 2). Male gametes tended to be in early stages of development where present, while female gametes were in more mature stage of development. Five (62.5%) of the corals identified as female displayed LD bands at the apex of the core, while 3 (37.5%) exhibited HD bands at their apex. Four (66.6%) of 6 males displayed HD bands at the apex of the core, while 2 (33.3%) exhibited LD bands at their apex. A Fisher's exact test determined that colony gender and the identity of the most recent band were independent ($p = 0.5921$, odds ratio = 3.04). Gender was not significantly related to TTL , E_0 , E_1 , or core length.

Apparent time difference comparisons

Values of ATD_P ranged from 0.07 months to 11.23 months with a mean (\pm SE) of 6.74 (\pm 0.52) months. Similarly, ATD_{O-T} ranged from 0.01 months to 11.41 months with a mean (\pm SE) of 6.26 (\pm 0.58) months, while ATD_{O-P} (untransformed) ranged from 0.07 months to 11.62 months with a mean (\pm SE) of 6.23 (\pm 0.61) months. The mean (\pm SE) difference between SST-derived and PAR-derived ATD s was 1.69 (\pm 0.03) months, and the difference

between predicted values of the models mirrored this shift (Fig. S4, ESM). The relative importance of predictors in both averaged mixed effect models supported the known influence of the physiological variables (TTL , E_0 , and E_1) from the Townsville model (1993) on ATD . In both models, tissue thickness had a relative importance of 0.95, having occurred in 19 of 26 component models in the top model set for ATD_{O-T} and 18 of 25 for ATD_{O-P} , while annual variation in extension had a relative importance of 0.94 in each average model. Extension rate had relative importance values of 0.84 and 0.83 in the SST-derived and PAR-derived models, respectively. Despite a clear effect of each variable in isolation, the three-way interaction of the Townsville variables had the lowest relative importance (0.33, ATD_{O-T} ; 0.34, ATD_{O-P}) and appeared in only two component models of each averaged model. No predictor or interactions between predictors in either averaged model significantly explained variation in ATD_O .

Effect size was examined to compare predictor variables that were measured on different scales (Fig. 3). Most effect size estimates were small and had 95% confidence intervals containing zero, indicating a small or uncertain effect on ATD_O (Fig. 3, Table S3, ESM). Furthermore, neither SST-derived nor PAR-derived ATD_M was significantly related to ATD_P by linear regression (SST: $p = 0.0668$, multiple

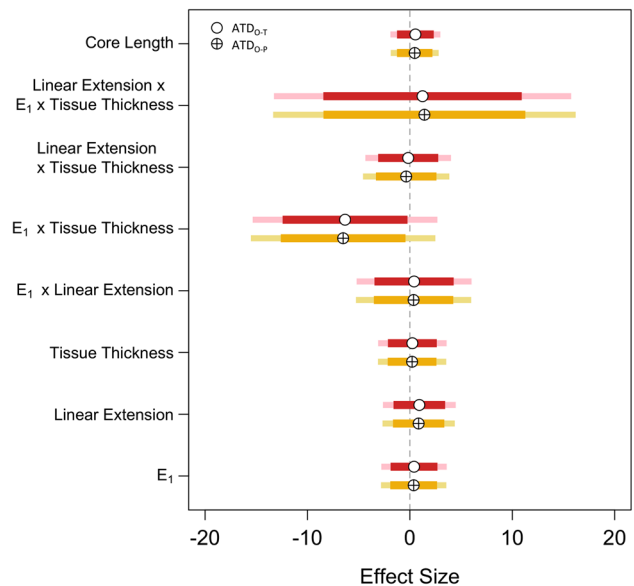


Fig. 3 Effect size of model predictors on observed apparent time difference derived from temperature (ATD_{O-T} , red bars) and light (ATD_{O-P} , gold bars): core length, annual variation in linear extension (E_1), mean extension rate (E_0), and thickness of the tissue layer (TTL). Most predictors had an effect size close to 0, with the exception of $E_1 \times TTL$, which was strongly negative but not significant (ATD_{O-T} : estimate = -6.3311, $p = 0.155$; ATD_{O-P} : estimate = -6.5177, $p = 0.142$). Open circles represent the point estimate, while darker and lighter bars represent 80 and 95% confidence intervals, respectively

$R^2 = 0.0982$; PAR: $p = 0.1058$, multiple $R^2 = 0.0773$; Fig. S4, ESM). No difference was found between ATD_O calculated using 5 yr versus only the most recent extreme (ATD_{O-T} : $p = 0.838$; ATD_{O-P} : $p = 0.852$).

Discussion

The present lack of a universal model of variability in coral banding presents challenges in interpreting coral growth records, reef responses to environmental change, and the reconstruction of past climate conditions. Despite an extensive body of literature that confirms the importance of seasonal variations in light and temperature in coral growth patterns (see Barnes and Lough 1996 for a review), the mechanisms by which these two basic drivers are differentially recorded within coral skeletons as well as the impacts of other environmental and physiological variables remain unclear. The development and application of a model that can characterize banding variability with high fidelity will (1) confer greater accuracy and resolution to current studies relying on density banding, (2) make possible the characterization of short-term responses in growth to acute disturbance events, and (3) enable recovery and interpretation of sub-seasonal proxy data contained within cores. The current study aimed to assess the capacity of an existing model to characterize variability in banding patterns for colonies of *S. siderea*, a resilient, Caribbean reef-building coral.

Nonsignificant correspondence between predicted and observed apparent time differences in the current study indicates that there may be undescribed factors, not identified herein, influencing the timing and appearance of banding in this species. While the models of ATD_O corroborate the importance of the three variables (TTL , E_0 , E_1) in the Townsville model, none of the additional variables (core length, reef zone, site) significantly explained ATD_O (Fig. 3). This may be due in part to the Townsville model's utilization of a single sine function to represent environmental drivers of banding (Taylor et al. 1993). Though a reasonable approximation for annual variations in light and temperature, a single sine function does not capture disagreements between the amplitudes or frequencies of the various environmental parameters that govern coral growth, nor any temporal mismatch between these (Knutson et al. 1972). The SST and PAR data examined herein revealed that light and temperature cycles in the Florida Keys are offset by approximately 2 months. However, the amount of variation in banding patterns explained by the core characteristics examined in the current study did not vary between the models relying on either SST or PAR. In reality, it is likely that the light and temperature cycles interact to exert control over banding, and future studies

should prioritize teasing apart the relative contribution of each rather than aggregating them into a single function. In addition, the spatial scale of analysis (FKRT-wide, Fig. 1) may limit our ability to firmly link environmental conditions with growth responses in *S. siderea* given the variation in environments observed across the study sites (Vega-Rodriguez et al. 2015).

The method used to calculate ATD in the current study was largely insensitive to specific extrema pairings. In other words, the level of variation in banding that was explained by each model was consistent whether using five within-core replicates or one, pairing matching extrema or opposite extrema, or quantifying ATD in relation to temperature or light. While the method used lends itself to the characterization of relative displacement between the environmental function and the corresponding density profile, it cannot definitively pair extrema in the environmental signal with the responding extreme in density. Future studies must prioritize the absolute pairing of extrema via alizarin staining or isotopic analysis to eliminate uncertainty about the true ATD presented in a given coral core.

A potential complication in our application of the Townsville model is that changes in skeletal architecture and the underlying mechanisms that give rise to differences in density over time may not be consistent across all scleractinian coral species. Several studies have sought to characterize the skeletal signature of banding but have been limited in scope to a single genus (frequently *Porites* spp.). Disparate results across studies suggest that growth strategies, specifically the mechanisms by which calcium carbonate is added to the basic skeletal matrix, may differ between and even within species (Macintyre and Smith 1974; Buddemeier and Kinzie 1975; Emiliani et al. 1978; Barnes and Devereux 1988; Dodge et al. 1993; DeCarlo and Cohen 2017). A notable difference between *S. siderea* and *Porites* spp., which were the basis for the Townsville model, is the ratio of TTL to E_0 . *Porites* spp. grow quickly relative to *S. siderea*, with annual extension rates of *Porites* spp. averaging 10–14 mm yr⁻¹ (Barnes and Lough 1992). In contrast, mean extension rate of the *S. siderea* colonies measured in the current study was closer to 3–4 mm yr⁻¹ despite roughly similar tissue thicknesses (5.2 and 6.4 mm for *Porites* spp. and *S. siderea*, respectively; Barnes and Lough 1992). Different ratios of tissue thickness to linear extension are expected to result in different levels of annual variation in density and may have other effects on banding timing and appearance (Taylor et al. 1993; Barnes and Lough 1996). This is due primarily to asynchrony in the two main processes contributing to bulk density, more specifically, the way in which variations in these two processes—extension and thickening—impact either the top or subsurface of the

colony at different times. Essentially, corals calcify throughout the depth of their tissue layers, thickening a skeletal framework that was already deposited via outward extension at the surface of the colony (Taylor et al. 1993; Barnes and Lough 1996). With low extension rates and thick tissue layers, ATD_{O} for corals in the present study may be exceptionally prone to distortion via this asynchrony. Future studies seeking to characterize banding across genera or species exposed to the same environmental conditions should aim to understand the full suite of physiological variables influencing banding and how each differentially responds to various environmental drivers within and between species.

Gender alone could not explain variations in ATD in the *S. siderea* cores analyzed in the current study (Fig. 2). Previous work has shown that the differences in energy required for reproduction can lead to differences in calcification (Leuzinger et al. 2003) and banding pattern (Carricart-Ganivet et al. 2013; Mozqueda-Torres et al. 2018). The lack of relationships herein may be due in part to the time of year at which tissue samples were collected. In *S. siderea*, spermaries are generally fully developed by June, while oocytes reach full development around July (Szmant 1986), which is 2–3 months later than our sampling trips in April. Furthermore, the sample size of our gender data was relatively small ($n = 14$), and spermaries, where present, tended to be in early stages of development (Szmant 1986). Consequently, any impact of reproduction on calcification resources, and therefore banding, was not readily inferable. Because energy demands for reproduction are seasonal and only present at maturity, the magnitude of impact on banding may not be uniform throughout the year (Szmant 1986) or even over the coral's lifetime (Hall and Hughes 1996). Further investigation into what physiological differences (e.g., extension, tissue thickness) may exist between male and female corals of different species and reproductive strategies (broadcast vs. brooders) will provide a basis for understanding their impact on banding timing in corals.

Though the annual nature of density bands has long been established (Knutson et al. 1972), constituent HD and LD bands do not necessarily contribute equally to observed linear extension (Barnes and Lough 1993, 1996). On average, the LD band accounts for $62 \pm 10\%$ of the width of the annual band (Barnes and Lough 1996). The current study found an average LD width of $45 \pm 0.7\%$ of the annual band, potentially suggesting less seasonality in extension rates in these corals. However, it is important to note that the proportional width of each semiannual band does not necessarily reflect the relative length of time over which each band is formed due to variations in intra-annual extension rates (Barnes and Lough 1993, 1996). Teasing apart the signal requires separating the true timing of

deposition from the resulting visual pattern. Our analysis is limited by the fact that linear extension was only measured on an annual scale, using the width of paired HD and LD bands. As a consequence, density profiles will have the greatest accuracy at a resolution greater than or equal to 1 yr. Without measurement of extension rates in situ or via fluorescent staining of the skeleton, temporal standardizations of the density profile that assume constant extension over the width of an annual band will systematically distort part or all of the profile (Barnes and Lough 1996). This has hitherto been a chronic and pervasive problem in banding studies (Barnes and Lough 1996). One promising remedy for this limitation is the direct measurement of seasonal extension rates through dissepiment spacing. Dissepiments—the thin, horizontal bulkheads upon which the living tissue layer rests within porous coral skeletons—have been demonstrated to deposit in sync with lunar cycles in *Porites* spp. (DeCarlo and Cohen 2017). Dissepiments may therefore offer a means of reliably tracking extension at monthly resolution in some species. While dissepiments have been observed in *S. siderea* and used to characterize their phenotypic plasticity (Foster 1977, 1979, 1980), authors of the current study are unaware of any work that has utilized dissepiments to quantify extension rates in this species.

In addition to conferring greater resolution to density profiles, quantification of seasonal extension rates will also allow for a greater understanding of the relative contribution of the extension and thickening processes to bulk skeletal density and variations therein. Abundant literature exists on the seasonal changes in skeletal architecture but lacks a uniform interpretation of the contributions of extension and thickening (see Macintyre and Smith 1974; Dodge et al. 1993; Barnes and Lough 1996). Even within the genus *Porites*, authors have come to different conclusions about the role of each process in band formation (e.g., Barnes and Devereux 1988; DeCarlo and Cohen 2017). Similar to the potential smearing influence of distinct (though correlated) environmental functions exerting influence over coral growth asynchronously, the single density profile in a core may be smeared by the effect of extension and thickening responding at the same time over different parts of the skeleton—extension adding to the top and thickening adding throughout the depth of the tissue layer (Taylor et al. 1993; Barnes and Lough 1996). In species like *S. siderea* with relatively slow growth rates, these effects may be even more subtle and difficult to detect. For example, the high ratio of tissue thickness to linear extension observed in the *S. siderea* cores from this study suggests that this species may routinely thicken the skeleton throughout a skeletal depth encompassing a full 24 months of linear extension. Consideration of these differences across species and genera could facilitate the

development of a more universally applicable model of coral banding.

The results of the current study highlight the continued need for mechanistic investigations into coral banding. Beyond its implications for the interpretation of proxy data and the improvements in resolution to be gained, elucidation of the physiological determinants of banding will help to characterize how corals will respond to continued environmental change and the resultant effects on growth. The poor correspondence between the Townsville model based on *Porites* spp. and our measurements of band timing in *S. siderea* does not necessarily indicate that the model fails to capture the majority of important variables in apparent time differences. Rather, individual variation within this species may be so great as to obscure any potential patterns or relationships. The challenge then becomes characterizing the factors contributing to variability in banding pattern at the level of the individual colony.

Overall, little is understood about how massive reef-building corals differentially record environmental signals in their skeleton. While physiological characteristics like tissue thickness and linear extension rate may explain some of the differences observed, these variables alone do not appear to capture the full range of predictors. Future research efforts should seek to characterize the full suite of variables governing banding. Quantification of these variables, together with expanded studies across a myriad of coral species, will promote the recovery of reliable proxy data from coral cores as well as crucial information about reef responses to environmental stress.

Acknowledgements We thank Hannah Aichelman, Lauren Speare, and Alyssa Knowlton for field assistance and tissue sample preparation. We also thank Adam St. Gelais for assistance with gender determination and the UNC Histopathology Core for their processing of tissue samples. Lastly, we thank Dr. Thomas M. DeCarlo for his thoughtful and thorough review. The data reported in this paper can be accessed at <https://www.bco-dmo.org/person/51711> or https://github.com/bebenson9/ATD_Ssiderea. The research was funded by the National Science Foundation grant OCE 1459522 to KDC.

Author contributions BEB, JPR, and KDC designed the study. BEB and JPR analyzed the data. JPR and KDC acquired permits and collected samples. CBB provided assistance with histological and statistical methods. All authors contributed to the writing of the manuscript.

Compliance with ethical standards

Conflict of interest On behalf of all authors, the corresponding author states that there is no conflict of interest.

References

- Barnes DJ, Devereux MJ (1988) Variations in skeletal architecture associated with density banding in the hard coral *Porites*. *J Exp Mar Bio Ecol* 121:37–54
- Barnes DJ, Lough JM (1992) Systematic variations in the depth of skeleton occupied by coral tissue in massive colonies of *Porites* from the Great barrier reef. *J Exp Mar Bio Ecol* 159:113–128
- Barnes DJ, Lough JM (1993) On the nature and causes of density banding in massive coral skeletons. *J Exp Mar Bio Ecol* 167:91–108
- Barnes DJ, Lough JM (1996) Coral skeletons: storage and recovery of environmental information. *Glob Chang Biol* 2:569–582
- Barnes DJ, Taylor RB, Lough JM (2003) Measurement of luminescence in coral skeletons. *J Exp Mar Bio Ecol* 295:91–106
- Bartón K (2013) MuMIn: Multi-model selection. R package version 1.40.0. <http://cran.r-project.org/web/packages/MuMIn/MuMIn.pdf>
- Bates D, Maechler A, Bolker B, Walker S (2015) Fitting Linear Mixed-Effects Models Using lme4. *Journal of Statistical Software* 67(1):1–48. <https://doi.org/10.18637/jss.v067.i01>
- Brown B, Le Tissier M, Howard LS, Charuchinda M, Jackson JA (1986) Asynchronous deposition of dense skeletal bands in *Porites lutea*. *Mar Biol* 93:83–89
- Buddemeier RW, Kinzie RA (1975) The chronometric reliability of contemporary corals. Growth rhythms and the history of the earth's rotation. Wiley, London, pp 135–146
- Buddemeier RW, Maragos JE, Knutson DW (1974) Radiographic studies of reef coral exoskeletons: rates and patterns of coral growth. *J Exp Mar Bio Ecol* 14:179–199
- Burnham KP, Anderson DR (1998) Model Selection and Inference. Springer, New York, New York, NY
- Cantin NE, Cohen AL, Karnauskas KB, Tarrant AM, McCorkle DC (2010) Ocean warming slows coral growth in the Central Red Sea. *Science* 329(5989):322–325
- Carricart-Ganivet JP, Vásquez-Bedoya LF, Cabanillas-Terán N, Blanchon P (2013) Gender-related differences in the apparent timing of skeletal density bands in the reef-building coral *Siderastrea siderea*. *Coral Reefs* 32:769–777
- Castillo KD, Ries JB, Weiss JM (2011) Declining coral skeletal extension for forereef colonies of *Siderastrea siderea* on the Mesoamerican Barrier Reef System, Southern Belize. *PLoS One* 6:e14615
- Castillo KD, Ries JB, Weiss JM, Lima FP (2012) Decline of forereef corals in response to recent warming linked to history of thermal exposure. *Nat Clim Chang* 2:756–760
- Comboul M, Emile-Geay J, Evans MN, Mirnateghi N, Cobb KM, Thompson DM (2014) A probabilistic model of chronological errors in layer-counted climate proxies: applications to annually banded coral archives. *Clim Past* 10:825–841
- DeCarlo TM, Cohen AL (2017) Dissepiments, density bands and signatures of thermal stress in *Porites* skeletons. *Coral Reefs* 36:749–761
- DeLong KL, Flannery JA, Poore RZ, Quinn TM, Maupin CR, Lin K, Shen C-C (2014) A reconstruction of sea surface temperature variability in the southeastern Gulf of Mexico from 1734 to 2008 C.E. using cross-dated Sr/Ca records from the coral *Siderastrea siderea*. *Paleoceanography* 29:403–422
- Dodge RE, Szmant-Froelich A, Garcia R, Swart PK, Forester A, Leder JJ (1993) Skeletal structural basis of density banding in the reef coral *Montastrea annularis*. *Oceanography Faculty Proceedings, Presentations, Speeches, Lectures*. 38
- Dodge RE, Vaisnys JR (1980) Skeletal growth chronologies of recent and fossil corals

- Emiliani C, Hudson JH, Shinn EA, George RY (1978) Oxygen and carbon isotopic growth record in a reef coral from the Florida Keys and a deep-sea coral from Blake Plateau. *Science* 202(4368):627–629
- Fischer AH, Jacobson KA, Rose J, Zeller R (2008) Hematoxylin and eosin staining of tissue and cell sections. *CHS Protoc* 2008(6):pdb.prot4986-pdb.prot4986
- Foster AB (1977) Patterns of small-scale variation of skeletal morphology within the scleractinian corals, *Montastrea annularis* and *Siderastrea siderea*. *Proceedings of the Third International Coral Reef Symposium* 2:409–415
- Foster AB (1979) Phenotypic plasticity in the reef corals *Montastrea annularis* (Ellis & Solander) and *Siderastrea siderea* (Ellis & Solander). *J Exp Mar Bio Ecol* 39:25–54
- Foster AB (1980) Environmental variation in skeletal morphology within the Caribbean reef corals *Montastrea annularis* and *Siderastrea siderea*. *Bull Mar Sci* 30:678–709
- Gelman A, Su Y (2018) arm: Data Analysis Using Regression and Multilevel/Hierarchical Models. R package version 1.10-1. <https://CRAN.R-project.org/package=arm>
- Glynn PW, Gassman NJ, Eakin CM, Cortes J, Smith DB, Guzman HM (1991) Reef coral reproduction in the eastern Pacific: Costa Rica, Panama, and Galapagos Islands (Ecuador): I. Pocilloporidae. *Mar Biol* 109(3):355–368
- Grueber CE, Nakagawa S, Laws RJ, Jamieson IG (2011) Multimodel inference in ecology and evolution: challenges and solutions: multimodel inference. *J Evol Biol* 24:699–711
- Guzmán H, Tudhope A (1998) Seasonal variation in skeletal extension rate and stable isotopic ($^{13}\text{C}/^{12}\text{C}$ and $^{18}\text{O}/^{16}\text{O}$) composition in response to several environmental variables in the Caribbean reef coral *Siderastrea siderea*. *Mar Ecol Prog Ser* 166:109–118
- Haberlah D, Williams MAJ, Halverson G, McTainsh GH, Hill SM, Hrstka T, Jaime P, Butcher AR, Glasby P (2010) Loess and floods: high-resolution multi-proxy data of Last Glacial Maximum (LGM) slackwater deposition in the Flinders Ranges, semi-arid South Australia. *Quat Sci Rev* 29:2673–2693
- Hall VR, Hughes TP (1996) Reproductive strategies of modular organisms: comparative studies of reef-building corals. *Ecology* 77:950–963
- Highsmith RC (1979) Coral growth rates and environmental control of density banding. *J Exp Mar Bio Ecol* 37:105–125
- Hounsfield GN (1973) Computerized transverse axial scanning (tomography): part 1. Description of system. *Br J Radiol* 46:1016–1022
- Hubbard DK, Scaturo D (1985) Growth rates of seven species of scleractinian corals from Cane Bay and Salt River, St. Croix, USVI. *Bull Mar Sci* 36:325–338
- Hurrell JW, Visbeck M, Busalacchi A, Clarke RA, Delworth TL, Dickson RR, Johns WE, Koltermann KP, Kushnir Y, Marshall D, Mauritzen C, McCartney MS, Piola A, Reason C, Reverdin G, Schott F, Sutton R, Wainer I, Wright D (2006) Atlantic climate variability and predictability: a CLIVAR perspective. *J Clim* 19:5100–5121
- Knutson DW, Buddemeier RW, Smith SV (1972) Coral chronometers: seasonal growth bands in reef corals. *Science* 177(4045):270–272
- Langebroek P, Bradshaw C, Yanchilina A, Caballero-Gill R, Pew C, Armour K, Lee S-Y, Jansson I-M (2012) Improved proxy record of past warm climates needed. *Eos (Washington DC)* 93:144–145
- Leuzinger S, Anthony KRN, Willis BL (2003) Reproductive energy investment in corals: scaling with module size. *Oecologia* 136:524–531
- Lough JM, Barnes DJ (1989) Possible relationships between environmental variables and skeletal density in a coral colony from the central Great Barrier Reef. *J Exp Mar Biol Ecol* 134:221–241
- Lough JM, Barnes DJ (1990) Intra-annual timing of density band formation of *Porites* coral from the central Great Barrier Reef. *J Exp Mar Biol Ecol* 135:35–57
- Lough JM, Barnes DJ (2000) Environmental controls on growth of the massive coral *Porites*. *J Exp Mar Biol Ecol* 245:225–243
- Lough JM, Barnes DJ, Taylor RB (1996) The potential of massive corals for the study of high-resolution climate variation in the past millennium. In: Jones PD, Bradley RS, Jouzel J (eds) *Climatic Variations and Forcing Mechanisms of the Last 2000 Years*:355–371. Springer Berlin Heidelberg, Berlin, Heidelberg
- Macintyre IG, Smith SV (1974) X-radiographic studies of skeletal development in coral colonies. In *Proc 2nd int coral Reef Symp* 2:277–287
- Mozqueda-Torres MC, Cruz-Ortega I, Calderon-Aguilera LE, Reyes-Bonilla H, Carricart-Ganivet JP (2018) Sex-related differences in the sclerochronology of the reef-building coral *Montastrea cavernosa*: the effect of the growth strategy. *Mar Biol* 165(2):32
- Nakagawa S, Freckleton RP (2011) Model averaging, missing data and multiple imputation: a case study for behavioural ecology. *Behav Ecol and Sociobiol* 65:103–116
- NASA Goddard Space Flight Center's Ocean Biology Processing Group (2018) Photosynthetically Available Radiation, Aqua MODIS, NPP, L3SMI, Global, 4 km, Science Quality, 2003-present (1 Day Composite). NOAA NMFS SWFSC ERD. <https://coastwatch.pfeg.noaa.gov/erddap/griddap/erdMHIpar01day.html> <https://doi.org/10.5067/aqua/modis/l3m/par/2018>
- R Core Team (2017). R: A language and environment for statistical computing. R Foundation for Statistical Computing, Vienna, Austria
- Reuer MK, Boyle EA, Cole JE (2003) A mid-twentieth century reduction in tropical upwelling inferred from coralline trace element proxies. *Earth Planet Sci Lett* 210:437–452
- Reynolds RW, Smith TM, Liu C, Chelton DB, Casey KS, Schlax MG (2007) Daily high-resolution-blended analyses for sea surface temperature. *J Clim* 20:5473–5496
- Smalley I, Fagg R (2015) John Hardcastle looks at the Timaru loess: climatic signals are observed, and fragipans. *Quat Int* 372:51–57
- St. Gelais AT, Chaves-Fonnegra A, Brownlee AS, Kosmynin VN, Moulding AL, Gilliam DS (2016) Fecundity and sexual maturity of the coral *Siderastrea siderea* at high latitude along the Florida Reef Tract, USA. *Invertebr Biol* 135:46–57
- Szmant AM (1986) Reproductive ecology of Caribbean reef corals. *Coral Reefs* 5:43–53
- Taylor RB, Barnes DJ, Lough JM (1993) Simple models of density band formation in massive corals. *J Exp Mar Biol Ecol* 167:109–125
- Vega-Rodriguez M, Müller-Karger F, Hallock P, Quiles-Perez G, Eakin C, Colella M, Jones DL, Li J, Soto I, Guild L, Lynds S, Ruzicka R (2015) Influence of water-temperature variability on stony coral diversity in Florida Keys patch reefs. *Mar Ecol Prog Ser* 528:173–186
- Verschuren D, Laird KR, Cumming BF (2000) Rainfall and drought in equatorial east Africa during the past 1,100 years. *Nature* 403(6768):410–414
- Wessel P, Smith WHF (1996) A global, self-consistent, hierarchical, high-resolution shoreline database. *J Geophys Res* 101(B4):8741–8743
- Williams M, Cook E, van der Kaars S, Barrows T, Shulmeister J, Kershaw P (2009) Glacial and deglacial climatic patterns in Australia and surrounding regions from 35,000 to 10,000 years ago reconstructed from terrestrial and near-shore proxy data. *Quat Sci Rev* 28:2398–2419

Winter A, Goenaga C, Maul GA (1991) Carbon and oxygen isotope time series from an 18-year Caribbean reef coral. *J Geophys Res* 96:16673

Wolff EW, Fischer H, Fundel F, Ruth U, Twarloh B, Littot GC, Mulvaney R, Röthlisberger R, de Angelis M, Boutron CF, Hansson M, Jonsell U, Hutterli MA, Lambert F, Kaufmann P,

Stauffer B, Stocker TF, Steffensen JP, Bigler M, Siggaard-Andersen ML, Udisti R, Becagli S, Castellano E, Severi M, Wagenbach D, Barbante C, Gabrielli P, Gaspari V (2006) Southern Ocean sea-ice extent, productivity and iron flux over the past eight glacial cycles. *Nature* 440(7083):491–496